Metabolomic changes in lactating multiparous naturally MAP-infected Holstein-Friesian dairy cows suggest changes in mitochondrial energy pathways

by Taylor, E.N., Beckman, M., Hewinson, G., Rooke, D., Sinclair, L.A. and Mur, L.A.J.

Taylor, E.N., Beckman, M., Hewinson, G., Rooke, D., Sinclair, L.A. and Mur, L.A.J. (2022) 'Metabolomic changes in lactating multiparous naturally MAP-infected Holstein-Friesian dairy cows suggest changes in mitochondrial energy pathways', *Research in Veterinary Science* 152, pp. 354 - 363

Research in Veterinary Science 152 (2022) 354–363

Contents lists available at ScienceDirect

Research in Veterinary Science

journal homepage: www.elsevier.com/locate/rvsc

Metabolomic changes in lactating multiparous naturally MAP-infected Holstein-Friesian dairy cows suggest changes in mitochondrial energy pathways

E.N. Taylor [a], M. Beckmann [a], G. Hewinson [b], D. Rooke [c], L.A. Sinclair [d], L.A.J. Mur [a,*]

[a] Aberystwyth University, Ceredigion, UK
[b] Centre of Excellence for Bovine Tuberculosis, Aberystwyth University, Ceredigion, UK
[c] ProTEM Services Ltd, West Sussex, UK
[d] Department of Agriculture and Environment, Harper Adams University, Newport, Shropshire, UK

ARTICLE INFO

Keywords:
Mycobacterium avium subspecies *paratuberculosis*
Metabolomics
Milk
Lactation
Mitochondria
Lactose

ABSTRACT

Mycobacterium avium subspecies *paratuberculosis* (MAP) is the causative organism of Johne's Disease, a chronic intestinal infection of ruminants. Infected cows begin shedding MAP within the asymptomatic, subclinical stage of infection before clinical signs, such as weight loss, diarrhoea and reduced milk yields develop within the clinical stages of disease. Herein, we examine the milk metabolomic profiles of naturally MAP-infected Holstein-Friesian cows. The study used biobanked milk samples which were collected 73.4 ± 3.79 (early lactation) and 143 ± 3.79 (mean ± SE) (mid-lactation) days post-calving from 5 MAP-infected and 5 control multiparous cows. The milk metabolome was assessed using flow infusion electrospray high-resolution mass spectrometry (FIE-HRMS) for sensitive, non-targeted metabolite fingerprinting. Metabolite fingerprinting assessments using partial least squares discriminate analyses (PLS-DA) indicated that lactation stage was a larger source of variation than MAP status. Examining each lactation stage separately for changes associated to MAP-infection status identified 45 metabolites, 33 in early lactation and 12 in mid-lactation, but only 6 metabolites were targeted in both stages of lactation. Pathway enrichment analysis suggested that MAP affected the malate-aspartate shuffle during early lactation. Pearson's correlation analysis indicated relationships between milk lactose concentrations in mid-lactation and 6 metabolites that were tentatively linked to MAP-infection status. The targeted metabolites were suggestive of wider changes in the bioenergetic metabolism that appear to be an acceleration of the effects of progressing lactation in healthy cows. Additionally, milk lactose concentrations suggest that MAP reduces the availability of lactose derivatives.

1. Introduction

Mycobacterium avium subspecies *paratuberculosis* (MAP) is the causative organism of Johne's Disease, a chronic intestinal infection of ruminants. Common routes of transmission include; colostrum, milk and faeces (Sweeney, 1996), in addition to in-utero and environmental reservoirs (Biemans et al., 2021). Calves aged under 6-months of age are most susceptible to MAP with approximately 75 % of calves exposed to MAP aged under 6-months old developing lesions indicative of MAP in later life (Windsor and Whittington, 2010). Following a prolonged incubation period of 2 to 5 years, cows begin shedding MAP in the asymptomatic, subclinical stage of infection followed by the development of clinical signs, such as weight loss, diarrhoea and reduced milk yields during the clinical stage (Whitlock and Buergelt, 1996).

MAP infections represent a substantial financial burden to dairy farmers with each MAP-infected cow linked to losses of £113, mainly though reduced milk yields and voluntary culling (Barratt et al., 2018). However, despite various regional programmes designed to control and reduce the prevalence of MAP being initiated as early as the 1920s (Benedictus et al., 2000), MAP is endemic across many countries, including Australia, Canada, Denmark, Netherlands, UK and USA (Geraghty et al., 2014).

A recent review examining the means used to control MAP highlighted the popularity of the milk ELISA test, with 10 out of 22 countries using individual milk ELISA tests and a further 6 using bulk milk ELISA tests (Whittington et al., 2019). However, quarterly testing is required to

* Corresponding author.
E-mail address: lum@aber.ac.uk (L.A.J. Mur).

https://doi.org/10.1016/j.rvsc.2022.09.001
Received 5 January 2022; Received in revised form 1 September 2022; Accepted 2 September 2022
Available online 8 September 2022

accurately assess the MAP status of cows due to the sensitivity and specificity ranges of the individual milk ELISA test at 21–61 % and 83–100 %, respectively (Nielson and Toft, 2008). Alternative, milk-based diagnostic tests include; F57 qPCR, IS900 qPCR and PMS phage-based assays. These methods exhibit sensitivities of 76 %, 94 % and 40 % and specificities of 85 %, 93 % and 49 %, respectively (Butot et al., 2019), but require further validation.

Metabolomics is the study of large numbers of metabolites found within cells, biofluids, tissues or organisms. Previous sera-based metabolomic analyses highlighted energy deficits (De Buck et al., 2014) and amino acid accumulations (Taylor et al., 2022; De Buck et al., 2014), in addition to increased lipid-metabolism (De Buck et al., 2014) and phosphatidylcholine biosynthesis (Taylor et al., 2022) within MAP-challenged Holstein-Friesian (HF) cattle. In agreement, sera-based metabolomic analysis of naturally MAP-infected HF cattle suggested elevated lipid metabolism and reduced energy intake (Tata et al., 2021). Furthermore, Taylor et al. (2021) identified 5 metabolites (leukotriene B4, bicyclo prostaglandin E2, itaconic acid, 2-hydroxyglutaric acid and N6-acetyl-L-lysine) capable of differentiating between naturally MAP-infected and healthy HF heifers from 1- to 19-months of age. This highlighted the potential of metabolomics, particularly flow infusion electrospray ionization high-resolution mass spectrometry (FIE-HRMS), to identify potential biomarkers for MAP.

Considering milk, non-MAP focused metabolomic studies have shown the impact of the negative energy balance in individual dairy cows in early lactation (Xu et al., 2018), subclinical *Streptococcus agalactiae* mastitis (Tong et al., 2019) and the impact of dietary treatments (Scano et al., 2020) on the milk metabolome. However, although milk-based ELISA tests are popular, the potential of milk samples to identify MAP-related metabolomic changes has yet to be explored.

Herein, we assessed the use milk metabolomic profiling to identify novel biomarkers for MAP using FIE-HRMS. Further, we examined how the stage of lactation affects the ability of metabolomic approaches to identify MAP-infected cattle, followed by correlation analysis to highlight relationships between milk composition parameters and metabolites associated to MAP-infection status.

2. Methods

2.1. Animal samples

Biobanked milk samples were sourced from Harper Adams University (HAU) and received local ethical approval from the HAU Animal Welfare and Ethical Review Body. Cows were sourced from HAU in their 2nd lactation onwards (range, 2 to 7), were matched according to diet and demonstrated no other health issues (Supplementary Table 1, 2). Early and mid-lactation were defined as 14 to 100 days post-partum and > 100 days post-partum, respectively (Hutjens, 2016). Thus, samples were collected by pooling milk from all udder quarters during a.m. and p.m. milkings at 73.4 ± 3.79 (early lactation) and 143 ± 3.79 (mid-lactation) (mean ± SE) days post calving from 5 MAP-infected and 5 control multiparous HF dairy cows. In total, 40 samples were collected, 1 AM and 1 PM sample/cow/stage of lactation. However, individual AM and PM samples from each cow at each stage of lactation were mixed in proportion to AM and PM milk yields. Therefore, 20 samples (1 sample/cow/stage of lactation) were stored at −20 °C until metabolite fingerprinting. Early lactation samples were collected between mid-October and mid-November 2019, mid-lactation samples were collected between mid-December 2019 and mid-January 2019.

Cows categorised as MAP-infected showed one or more positive milk ELISA tests in their previous lactation, but the control group had negative milk ELISA results throughout all lactations. All cows were routinely MAP tested every 3 months using the IDEXX milk ELISA (NMR, Wolverhampton, UK). MAP faecal culture tests were conducted by the Animal and Plant Health Agency (Starcross, Exeter) using paraJEM™ growth media (Treks Diagnostic) and absence of MAP shedding was confirmed by Ziehl Neelsen (ZN) staining 121 ± 4.9 days post-calving. All cows, from both experimental classes, were MAP faecal culture negative and asymptomatic.

2.2. Untargeted metabolite fingerprinting by flow infusion electrospray ionization high resolution mass spectrometry (FIE-HRMS)

Milk samples were stored at −20 °C during the collection period before being stored at −80 °C for long-term storage prior to metabolomic analysis. Milk was prepared using the method described by Beckmann et al. (2008) with amendments. Once defrosted, 500 uL of raw milk were pipetted into a 2 mL microcentrifuge tube. Next, each 2 mL microcentrifuge tube was centrifuged at 22000 x*g* at 4 °C for 8 min and 200 uL of skimmed milk pipetted into 1520 μL pre-chilled solvent mix (methanol/chloroform [4/1 *v*/v]) containing 1 micro-spoon of glass beads (<160 μM glass beads [Sigma-Aldrich Ltd., Gillingham, UK]). Samples were then vortexed for 5 s, shaken for 15 min at +4 °C and kept at −20 °C for 20 min. Following centrifugation at 22000 x*g* and 4 °C for 5 min, 100 μL of the milk supernatant were transferred into mass spectrometry vials along with 100 μL methanol/water [70/30 v/v]. Samples were stored at −80 °C until analysis using FIE-HRMS. For each sample, 20 μL were injected into 70% water/ 30% methanol at a flow of 60 μL per minute, using a Surveyor flow system into a Q Exactive plus mass analyser instrument with a UHPLC system (Thermo Fisher Scientific©, Bremen, Germany). Data acquisition for each sample was in alternating the positive and negative ionization modes, throughout four different scan mass-ion (*m/z*) ranges (15–110 *m/z*, 100–220 *m/z*, 210–510 *m/z*, 500–1200 *m/z*) with an acquisition time of 2 min. Data were normalised to total ion counts. The derived data matrices are available at https://data.mendeley.com/datasets/2gsj2krvzb/1

2.3. Statistical analysis

Metabolomic data were analysed using MetaboAnalyst 4 (Chong et al., 2019). Data were subjected to interquartile range-based filtering, $\log_{10}$ transformations and Pareto scaling. Variables of importance for the projection (VIP) scores (>1) in partial least squares–discriminant analyses (PLS-DA) were used to indicate *m/z* values which discriminated between experimental classes in early and mid-lactation. Cross validation based on a Leave-One-Out Cross-Validation (LOOCV), indicated that PLS-DA did not overfit the data. Two-way ANOVA, corrected for false discovery rates (FDR), assessed the impact of MAP status and stage of lactation on *m/z* values with a VIP score > 1. Area under the curve (AUC) assessments based on sensitivity and specificity estimates, were used to suggest the accuracy of the targeted *m/z*. Major sources of variation were displayed using unsupervised hierarchical clustering analysis (HCA). Significant *m/z* were identified based on accurate mass (+/− 5 ppm) using the DIMEdb database (https://dimedb.ibers.aber.ac.uk/) based on their ionised masses, molecular formulae and the Bovine Metabolome Database (Foroutan et al., 2020). All isotopes/adducts were considered in deriving the identifications. Metabolite set enrichment analysis (MSEA) using over representation analysis (ORA) was used to highlight key pathways and biological patterns. Milk yield and milk composition was analysed by paired t.test using Genstat version 18 (VSN International Ltd., Oxford, UK). Correlation analyses between identified metabolites, milk yield and composition were based on Pearson's coefficients.

3. Results

Following FIE-HRMS, PLS-DA was used to assess the milk metabolite profiles of MAP-infected and control cows in early and mid-lactation (Fig. 1). Comparisons between all of the experimental classes indicated that lactation stage was by far the greater source of variation, compared to MAP status (Fig. 1a). However, when the different stages of lactation were considered separately, PLS-DA could discriminate

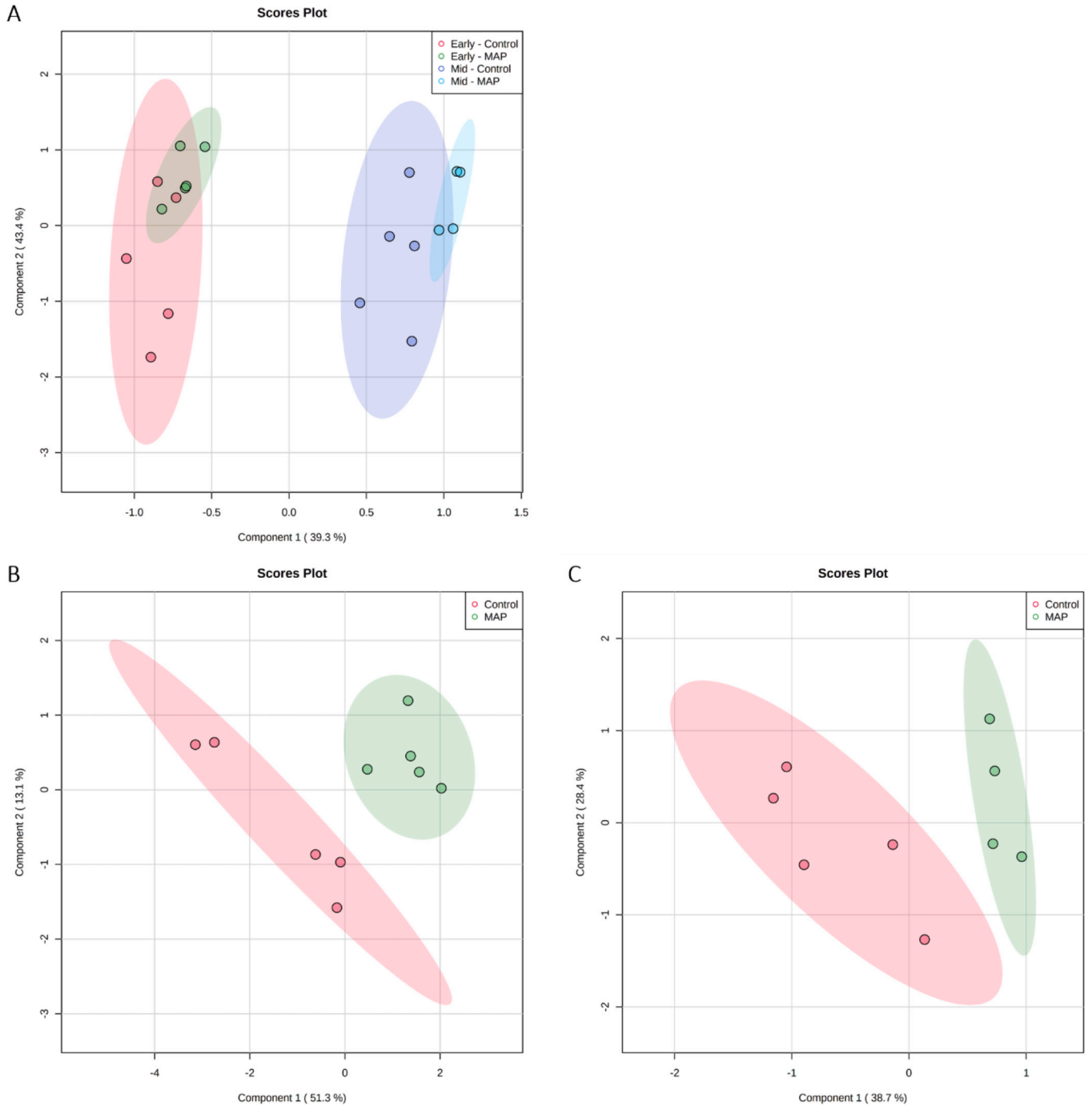

Fig. 1. Partial least-squares discriminant analysis (PLS-DA) for milk from MAP-infected and control cattle in A early (73.4 ± 3.79 days post-calving) and mid-lactation (143 ± 3.79 days post-calving) B early lactation only and C late lactation only in the mixed ionization mode. The ellipses represent 95% confidence intervals for each group.

between MAP-infected and control cows, with no overlapping of 95 % confidence intervals (Fig. 1b, Fig. 1c, Supplementary Fig. 1 and 2). Even if variation between individual cows is considered, samples obtained from the control cows were more variable than MAP-infected cows, irrespective of lactation period (Fig. 1b and Fig. 1c). The multivariate VIP scores from Fig. 1b and Fig. 1c as well as AUC scores of >0.6 (the minimum for acceptance) were used to target *m/z* linked to MAP infection (Table 1). A total of 45 *m/z* could differentiate between MAP-infected and controls cows within either early or mid-lactation. HCA and heatmaps successfully clustered the experimental groups in early lactation only, indicating that the identified metabolites could clearly differentiate between MAP-infected and control cows in early lactation (Fig. 2a) but less clearly for mid lactation (Fig. 2b), although considerable variation between the cows of each experimental class was noted. Of the 45 metabolites, only 6 metabolites were common to both lactation sample points, with most found at early lactation i.e. 33 early and 12 mid lactation (Table 1). Of the 6 common metabolites, (2-butenoic acid, 2-methylpentatnoic acid, 6-methylpentanoic acid, galactonic acid, glutamic acid and glycerol 1-acetate) all except 2-butenoic acid exhibited the same direction of change in early and mid-lactation (Fig. 3a). However, the relative levels of these metabolites appeared to differ with each stage of lactation. Indeed, univariate assessments based

Table 1
Metabolites differentiating between MAP-infected and control cattle.

Class	Subclass	Metabolite	Lactation	Mode	AUC	VIP Score	Log2 (FC)
Carboxylic acids and derivatives	Amino acids, peptides, and analogues	Alanine	Early	Negative	0.96	1.435	−0.630
		Aspartic acid	Early	Negative	0.72	1.267	−0.530
		Creatine	Early	Positive	0.88	1.216	−0.379
		Glutamic acid	Early	Negative	0.80	1.405	−0.736
	Tricarboxylic acids and derivatives	Homocitric acid	Early	Negative	0.84	1.153	−0.455
		cis-Aconitic acid	Early	Negative	0.88	1.151	−0.469
		Citric acid	Early	Negative	0.92	1.392	−0.643
Diazines	Pyrimidines and pyrimidine derivatives	Orotic acid	Early	Negative	0.84	1.143	−0.567
		Uracil	Early	Negative	0.84	1.291	−0.670
Fatty Acyls	Fatty acid esters	Acetylcarnitine	Early	Positive	0.64	1.459	0.859
		Dodecanoylcarnitine	Early	Positive	0.88	1.566	0.561
	Fatty acids and conjugates	10-Octadecenoic acid	Early	Negative	0.76	1.317	0.850
		2-Butenoic acid	Early	Negative	0.96	1.264	−0.503
		2-Methylpentanoic acid	Early	Negative	0.64	1.408	1.885
		3-Dehydroxycarnitine	Early	Positive	0.68	1.140	−0.350
		6-Methylheptanoic acid	Early	Negative	0.64	1.299	1.544
		Capric acid	Early	Negative	0.72	1.403	1.580
		Itaconic acid	Early	Negative	0.92	1.123	−0.417
		Pentadecanoic acid	Early	Negative	0.84	2.039	1.600
		Stearic acid	Early	Negative	0.92	1.144	0.524
Furans	Furoic acid and derivatives	3-Furoic acid	Early	Negative	0.92	1.423	−0.688
Glycerolipids	Monoradylglycerols	Glycerol 1-acetate	Early	Negative	0.84	1.335	−0.564
	Triradylcglycerols	TG(8:0/10:0/10:0)	Early	Positive	0.68	1.239	0.473
		TG(8:0/12:0/12:0)	Early	Positive	0.80	1.084	0.316
		TG(8:0/13:0/12:0)	Early	Positive	0.68	1.447	0.571
Hydroxy acids and derivatives	Beta hydroxy acids and derivatives	2-Deoxypentonic acid	Early	Negative	0.88	1.074	−0.434
		Malic acid	Early	Negative	0.84	1.443	−0.793
	Medium-chain hydroxy acids and derivatives	Galactonic acid	Early	Negative	0.84	1.209	0.500
	Short-chain hydroxy acids and derivatives	2-Hydroxyglutaric acid	Early	Negative	0.76	1.061	−0.485
Organic sulfuric acids and derivatives	Arylsulfates	4-ethylphenylsulfate	Early	Negative	0.92	1.539	−0.709
Organooxygen compounds	Alcohols and polyols	Pantothenic acid	Early	Negative	0.88	1.289	−0.534
	Carbohydrates and carbohydrate conjugates	Glucuronic acid	Early	Negative	0.88	1.144	−0.522
		Beta-N-Acetylglucosamine	Early	Negative	0.92	1.835	−1.009
Carboxylic acids and derivatives	Amino acids, peptides, and analogues	Glutamic acid	Mid	Negative	0.65	1.014	−0.393
		Valine	Mid	Positive	0.80	1.087	−0.359
	Carboxylic acids	Propynoic acid	Mid	Negative	0.80	1.510	0.628
	Dicarboxylic acids and derivatives	Glutaric acid	Mid	Negative	0.80	1.241	−0.480
	Tricarboxylic acids and derivatives	1,2,3-Propanetricarboxylic acid	Mid	Negative	0.70	1.076	0.517
		2,3-Methylenesuccinic acid	Mid	Negative	0.90	1.580	0.632
Fatty Acyls	Fatty acids and conjugates	2-Butenoic acid	Mid	Positive	0.85	1.088	0.391
		2-Methylpentanoic acid	Mid	Negative	0.75	1.412	1.108
		6-Methylheptanoic acid	Mid	Negative	0.75	1.218	0.819
Glycerolipids	Monoradylglycerols	Glycerol 1-acetate	Mid	Negative	0.75	1.190	−0.381
Glycerophospholipids	Glycerophosphocholines	Glycerophosphocholine	Mid	Negative	0.90	1.601	0.588
Hydroxy acids and derivatives	Medium-chain hydroxy acids and derivatives	Galactonic acid	Mid	Negative	0.85	1.407	0.501

on two-way ANOVA (corrected for FDR) suggested that only glycerol-1-acetate changed significantly with MAP status but also with lactation (Supplementary Table 3). The cause of this weak association with MAP infection for these biomarkers was suggested by considering the accumulation patterns of glycerol-1-acetate. This showed that the metabolite increases associated to MAP-infection status were higher than the respective controls at each sampling point; but, crucially, control mid-lactation levels were not significantly different to MAP-infected samples from the early lactation time point (Fig. 3b). This suggests that MAP associated changes were similar to those occurring at a later lactation stage in uninfected heifers.

Considering the types of metabolites that tended to change in response to MAP (Table 1), fatty acyls, carboxylic acids and derivatives classes were dominant. Fatty acyls accounted for a third of the identified metabolites, the direction of change varied in early lactation but decreased consistently in mid-lactation. In contrast, carboxylic acids and derivative levels consistently increased in early lactation but the direction of change varied in mid-lactation. The identified metabolites were analysed based on MSEA using ORA to link them to biological pathways. This highlighted the effect of MAP on the malate-aspartate shuttle in the mitochondria in early lactation in the negative ionization mode ($p < 0.05$) (Fig. 4 and Supplementary Fig. 3). Interestingly, the malate-aspartate shuttle was the most enriched pathway in mid-lactation in the negative ionization mode too, but these changes were non-significant ($p > 0.05$) (Supplementary Fig. 4, 5 and 6).

Examining milk composition parameters, MAP-infected cows tended ($p = 0.054$) to have lower milk lactose concentrations (g/kg) in mid-lactation (Supplementary Table 4). Pearson's correlation analysis examined the relationship between milk lactose concentrations (g/kg) and those metabolites that changed mid-lactation. In total, 6 metabolites were correlated to lactose concentrations ($-0.4 <$ correlation coefficient >0.4); 5 positively and 1 negatively. These metabolites were 2-methylpentanoic acid, 2, 3-methylenesuccinic acid, galactonic acid, glutaric acid, glycerol 1-acetate and propynoic acid (Fig. 5 and Supplementary Fig. 7).

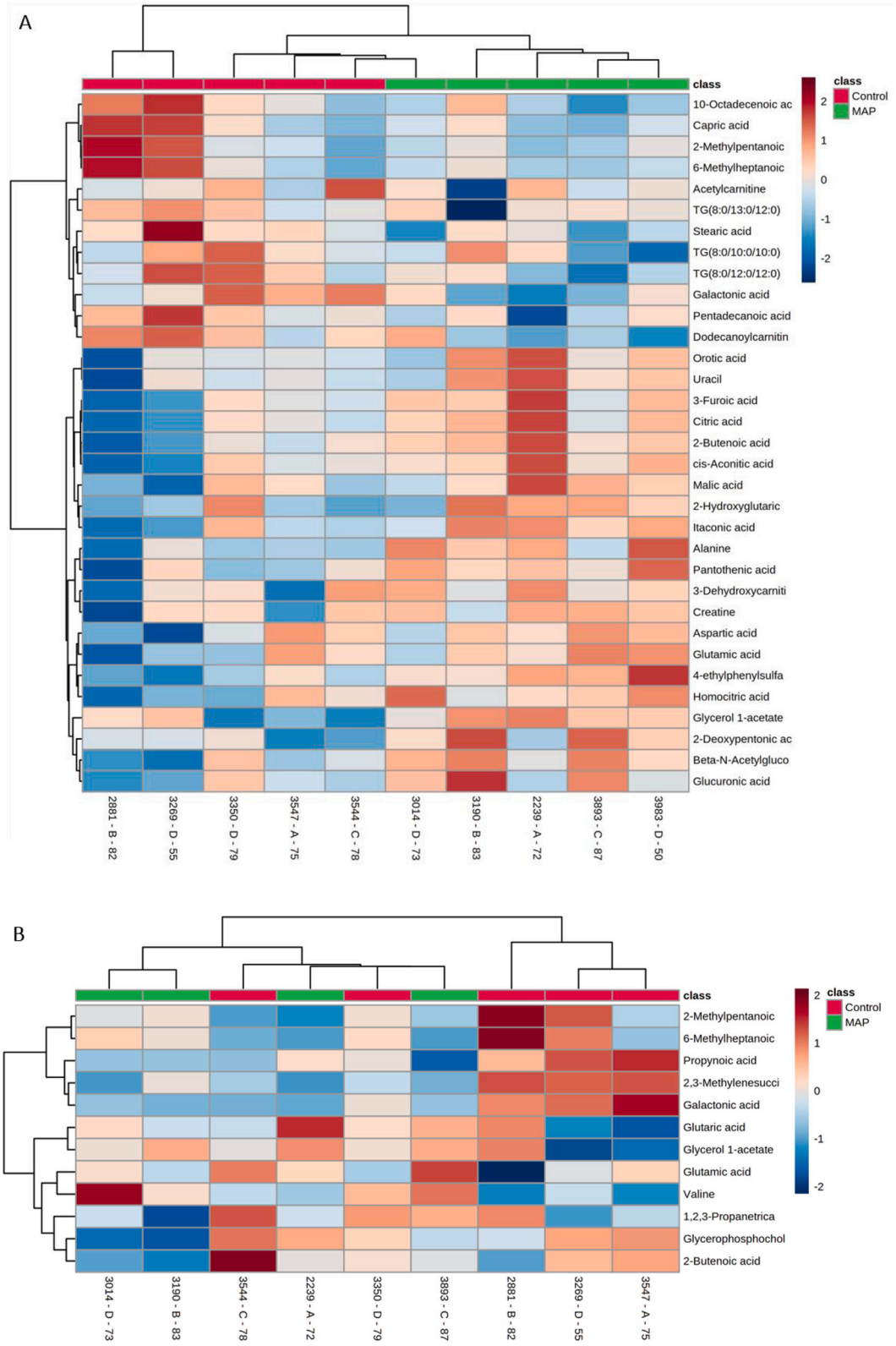

Fig. 2. Major metabolite changes differentiating between milk from MAP-infected and control cattle between in A early and B mid-lactation.

4. Discussion

The financial impact of MAP infections on dairy farmers (Barratt et al., 2018) and detection of MAP in pasteurised milk samples (Gerrard et al., 2018) is making the accurate and sensitive detection of MAP in milk increasingly important. This interest is also being driven by a possible link between MAP and Crohn's Disease (McNees et al., 2015). Previous serum focused metabolomic studies have highlighted changes in energy-related pathways and lipid-metabolism (De Buck et al., 2014; Tata et al., 2021), but the potential of milk metabolomic profiling is yet

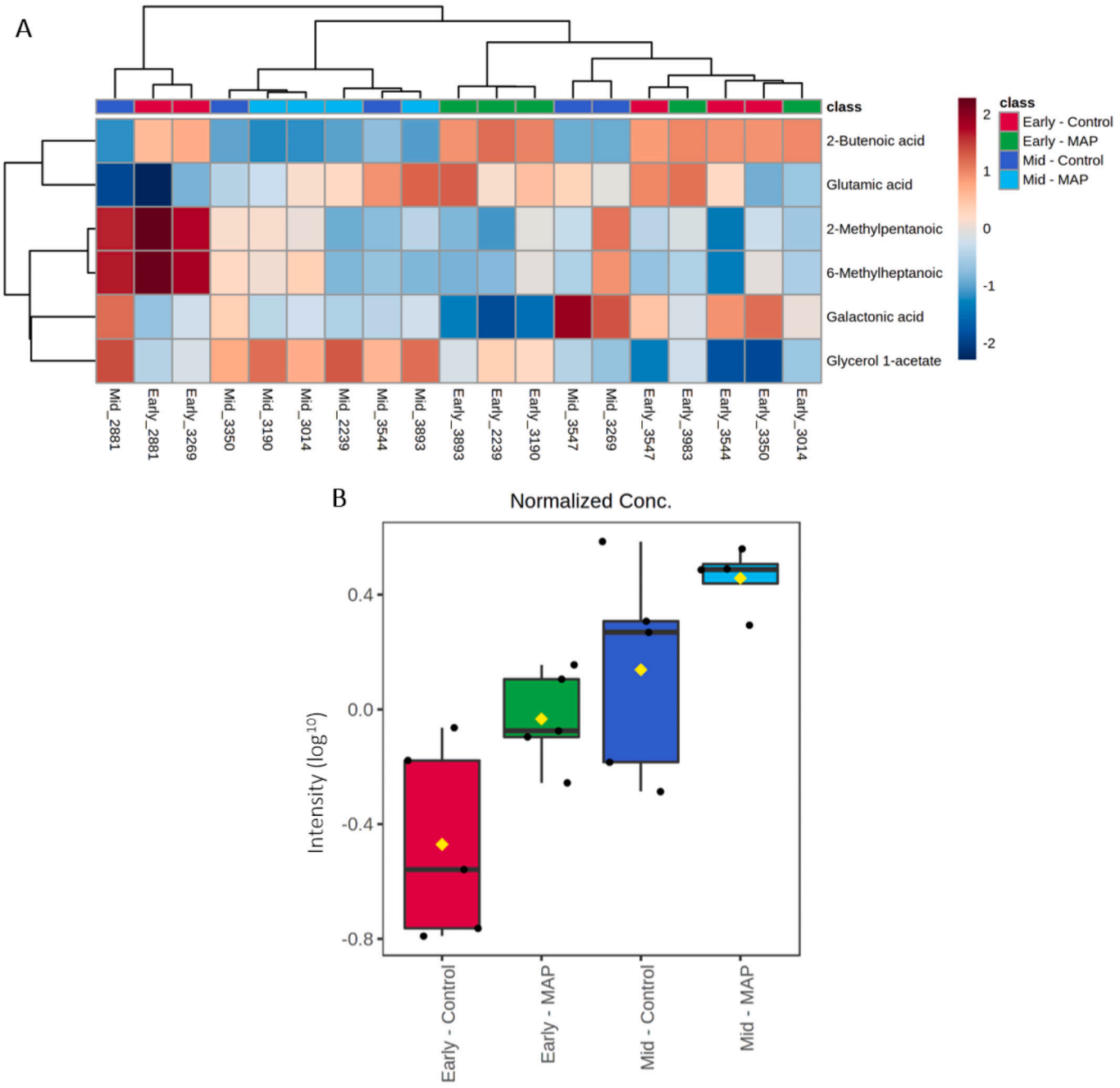

Fig. 3. A Hierarchical cluster analysis of metabolites affected by MAP (VIP score > 1) within MAP-infected and control cattle during early and mid-lactation B boxplots showing the effect of the stage of lactation on glycerol 1-acetate levels. Early = early lactation, mid = mid lactation.

to be explored. If metabolite changes could be detected in milk, these could represent biomarkers with the potential to be developed into a milk-based MAP diagnostic test. Additionally, in contrast to sera or plasma-based diagnostic tools, milk sampling is non-invasive and could be conducted by farmers. It was therefore, important not only to detect MAP responsive metabolites but also to define how these changed during lactation. This influenced our experimental design, which included milk sampling of MAP-ELISA positive cows at two stages of lactation.

The results of our FIE-HRMS assessment and multivariate statistical analyses identified 45 metabolites that were associated to MAP-infection status. Of these, only 6 MAP responsive metabolites were common to both early and mid- lactation stage. Such variability in metabolites with lactation was also observed in other, non-MAP related studies. Thus, Xu et al. (2018), attempted to use 10 milk metabolites to model energy balance at 2- and 7-weeks post-partum but only 5 metabolites were present at both timepoints. Moreover, the levels of the 6 metabolites common to early and mid-lactation were affected by time, as shown by glycerol 1-acetate (Fig. 3b). In the case of De Buck et al. (2014) who examined sera metabolomics in MAP-inoculated calves aged from 2-weeks to 17-months of age, these changes were thought to be attributable to growth and development. Further, considering the causes of this variation, in early lactation, cows enter negative energy balance in response to a sudden increase in glucose, amino acids and fatty acids requirements (Bell, 1995). It seems likely that this energy balance change could be a common response to MAP infection and early lactation stage, so that obtaining MAP-specific metabolite biomarkers were difficult to identify (Table 1). Interestingly, serum ELISA and faecal culture MAP diagnostic tests show decreased sensitivity as lactation

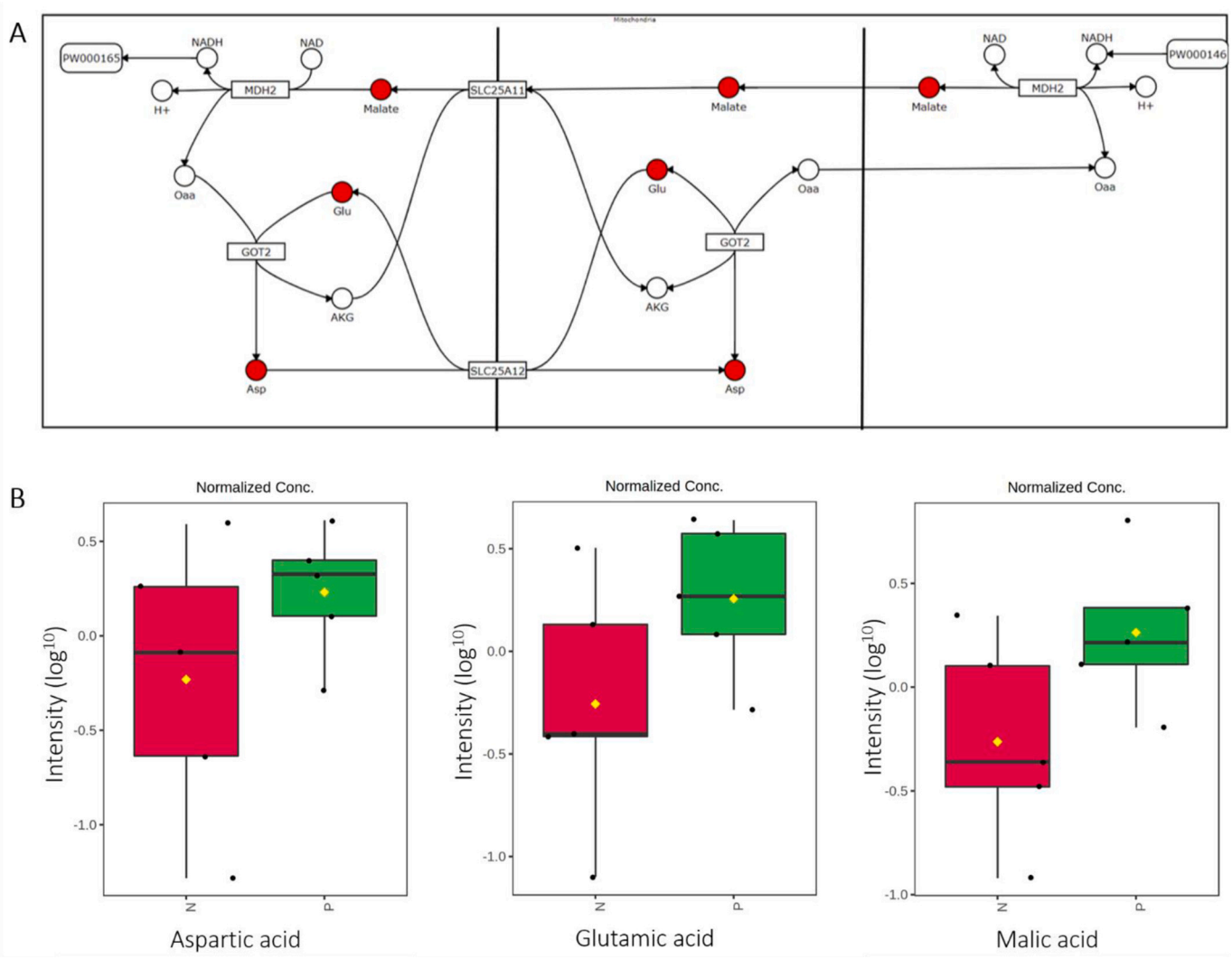

Fig. 4. A Metabolites set enrichment analysis (MSEA) using over representation analysis (ORA) demonstrates the effect of MAP on the malate-aspartate shuttle pathway in the mitochondria in early lactation, affected metabolites (VIP score > 1) are highlighted in red, and B boxplots showing the effects of MAP infection on aspartic acid, glutamic acid and malic acid levels. N = control, P = MAP-infected. (For interpretation of the references to colour in this figure legend, the reader is referred to the web version of this article.)

progresses (Stabel et al., 2014). In contrast, milk ELISA tests generally display increased sensitivity as lactation progresses (Nielson and Toft, 2012) and a positive energy balance is restored. Further metabolomic assessments with more time points are required to resolve how metabolomic changes associated with MAP-infection status could be related to the lactation cycle.

We recognise that a larger sample size with additional time points would improve the power of this pilot study. Considering the specificity of the detected metabolite changes, there was continuous cattle health monitoring throughout the study (such as verifying udder health through biweekly milk somatic cell count (SCC) (log_{10}/mL) assessments), suggesting a specificity for MAP infections. Further, many of the metabolomic changes associated with a positive MAP-infection status have been previously identified within sera collected from naturally MAP-infected heifers, including itaconic acid and 2-hydroxyglutaric acid. Crucially, these metabolites were significantly elevated in MAP-infected cattle aged between 1-month and 19-months of age, compared to control cattle (Taylor et al., 2021). This stated some of our MAP associated metabolites have been also seen in a metabolomic assessment of mastitis infection (Hu et al., 2021). Indeed, out of 45 identified metabolites in this MAP study, 5 have been previously linked to mastitis. For example, alanine was identified in milk samples collected from cattle with clinical mastitis infections (Luangwilai et al., 2021), and in our current MAP study. Such observations highlight the importance of the SCC assessments in reducing the possibility of mastitis complicating our observations. However, definitive exclusion of co-infection with such as *Mycobacterium bovis,* would help establish the specificity of identified metabolites. Therefore, although further studies examining the metabolomic effects of infection, particularly *M. bovis*, on the bovine metabolome are required. These should also aim to derive multiple metabolites linked to MAP-infection status of cattle, in order to improve the specificity of metabolite panels (Zhang et al., 2020).

4.1. *The possible role of MAP in mitochondrial bioenergetics*

Many of the MAP-related metabolites identified in early lactation have roles within mitochondrial bioenergetics as the MSEA analyses targeted the malate-aspartate shuttle (Fig. 4). During glycolysis, the malate-aspartate shuttle facilitates the transport of electrons across the inner mitochondrial membrane for oxidation phosphorylation (Ying, 2006). In the cytosol, malate dehydrogenase catalyses the formation of malate and NAD+ from oxaloacetate and NADH (Borst, 2020). Malate then crosses the inner mitochondrial membrane via the malate-α-keto-glutarate-transporter using bidirectional transfer, so a higher

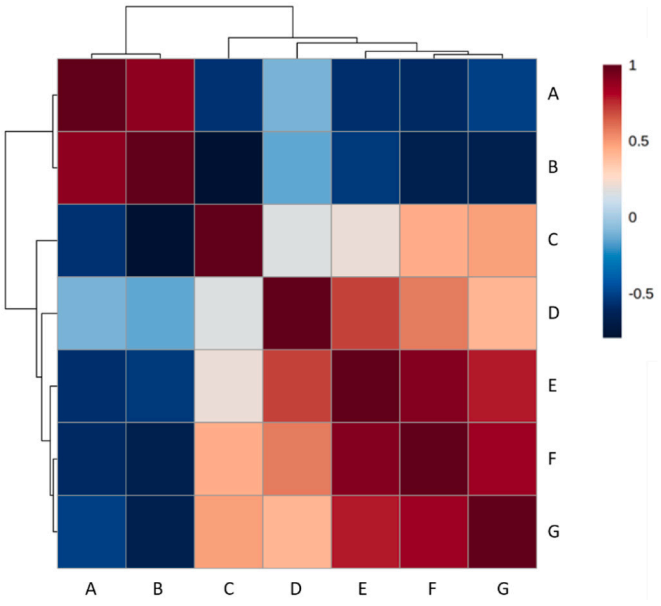

Fig. 5. A heatmap of the Pearson's correlation coefficients produced by comparing metabolites significantly affected by MAP-infected and control cattle with milk lactose (g/kg) and lactose yield (kg/day) in mid-lactation. Whereby, A = Glutaric acid, B = Glycerol 1-Acetate, C = Lactose (g/kg), D = 2-Methylpentanoic acid, E = 2,3-Methylenesuccinic acid, F = Galactonic acid, G = Propynoic acid. Positive correlations are shown in red, negative correlations are shown in blue. (For interpretation of the references to colour in this figure legend, the reader is referred to the web version of this article.)

concentration of electrons in the cytosol is crucial (Safer et al., 1970). In the mitochondrial matrix, malate dehydrogenase catalyses the reformation of oxaloacetate and NADH from malate and NAD^+ (Borst, 2020). The levels of affected metabolites (aspartic acid, glutamic acid and malic acid) increased within MAP-infected cows (Fig. 4b). De Buck et al. (2014) also reported increased aspartate and glutamine, suggesting that MAP-infected cows exhibit higher energy demands (Ying, 2006). This bioenergetic link for our metabolites associated with MAP-infection status may be the reason that for the variation over the lactation/developmental periods.

Xu et al. (2018) employed metabolomic analysis to differentiate between the milk metabolite profiles of cows 2- and 7-weeks postpartum that could predict the energy balance of individual cows. Likewise, Xu et al. (2020) used metabolomic analysis to compare energy balance and the metabolite profiles of milk and plasma from early lactation dairy cows. Interestingly, in our study, some of these identified metabolites also differentiated between milk samples from cows with a positive MAP-infection status and control cows; aspartic acid, carnitine, citric acid, creatine and glutamic acid (Table 1). Carnitine and citric acid account for 8.6% and 8.5% of the energy balance variation in early lactation. Citric acid, aspartate and glutamate are crucial components of the tricarboxylic acid (TCA) cycle (Martínez-Reyes and Chandel, 2020). Thus, these findings reinforce the link between MAP on energy-related pathways and therefore, the difficulty in identifying milk metabolomic changes associated with MAP-infection status which are not influenced by the energy balance of the host.

It is possible that these changes in mitochondrial metabolism, at least partially, reflect interactions between MAP and macrophages. Transcriptome profiling of MAP-challenged primary monocyte-derived macrophages at 1, 4, 8, and 24 h post-challenge highlighted that MAP-infected macrophages promoted an immunometabolic shift to aerobic glycolysis (Ariel et al., 2020). Therefore, the upregulation of the malate-aspartate shuttle may reflect the activation of macrophages. Transcriptome profiling has suggested that monocytes derived from cattle with a positive MAP-infection status can differentiate into mixed M1/M2 macrophage phenotypes (Ariel et al., 2020). However, determining the phase of these macrophages in our study was not possible. Likewise, the examination of molecular markers and release of effector agents within experimentally MAP-challenged cattle also reported mixed M1/M2 macrophage phenotypes (Thirunavukkarasu et al., 2015). In line with these observations, metabolomically, the *M. tuberculosis* elicited M1 state is associated with increases in glycolytic enzyme activity to promote the glycolytic flux, leading to increases in pyruvate and lactate within macrophages. The M2 phase is typified by increased citrate levels and the subsequent build-up of fatty acids as lipid droplets. MAP-infected cows showed increased citrate and the citrate derivative, itaconic acid (Fig. 2a) in early lactation. Itaconic acid is mainly produced by M1 macrophages and has been shown to inhibit *M. tuberculosis* growth in mice (Micheluccia et al., 2013). However, increases in glutamic acid throughout lactation (Fig. 2a) could be indicative of M2 polarization (Vrieling et al., 2020). Thus, our study supports previous studies (Ariel et al., 2020; Thirunavukkarasu et al., 2015) by suggesting that M1 and M2 macrophage phenotypes could be present simultaneously within MAP-infections.

4.2. The influence of MAP on milk lactose in mid-lactation

As bioenergetic metabolism was being affected by both the stage of lactation and MAP infection, we assessed how these could be reflected in milk composition parameters. Our assessments suggested that MAP-infected cows exhibited a trend ($p = 0.054$) of lower milk lactose concentrations in mid-lactation (Supplementary Table 4). Similarly, Donat et al. (2014), reported significant decreases in lactose concentrations (%), in addition to significant ($p < 0.05$) reductions in milk yield (kg) and milk protein (%) in MAP culture positive cows. Likewise, Jurkovich et al. (2016) observed a trend of lower lactose (%) ($p = 0.077$) and milk yields (L) ($p = 0.074$), as well as significantly ($p < 0.05$) higher fat concentrations (%) in milk from MAP faecal PCR positive cows. Our observation that only lactose concentrations were reduced in MAP-infected cows may reflect that, although the cows were milk ELISA positive, their MAP faecal culture results were negative. Nevertheless, milk lactose concentrations in mid-lactation were correlated ($-0.4 <$ correlation co-efficient >0.4) to 6 of the targeted MAP responsive metabolites (Fig. 5 and Supplementary Fig. 7). Lactose is synthesized from glucose and uridine diphosphate (UDP)-galactose in the Golgi apparatus (Costa et al., 2019). Propionoic acid is converted into glucose (Aschenbach et al., 2010) and UDP-galactose is derived from UDP-glucose via the enzyme UDP-glucose-4-epimeras (Frey, 1996). In line with this, galactonic acid and propynoic acid (an unsaturated propionate analog) levels were decreased in MAP-infected cows (Fig. 2) and display positively correlation with lactose (Fig. 5). In contrast, De Buck et al. (2014) reported notable increases in propionate and glutamate (the conjugate acid of galactonic acid) levels within sera from MAP-inoculated male HF cattle aged from 2-weeks to 17-months. Nevertheless, our data suggests that MAP indirectly decreases the availability of glucose and UDP-galactose for lactose synthesis.

5. Conclusion

Metabolomic analysis of milk samples from MAP-infected and control cows during early and mid-lactation using untargeted FIE-MS suggested that metabolomic changes associated to MAP-infection status could be observed. However, the identified metabolites appeared to be correlated with changes in bioenergetic metabolism and lactation-associated changes confounded the long-term detection of MAP. The findings of this pilot study are preliminary, future work could focus on identifying metabolites at additional time points throughout lactation and correlating these metabolites to milk energy output. This could also indicate better MAP-infection status discriminatory metabolites in milk that could serve as biomarkers.

Research data

The datasets used and/or analysed during the current study can be found at https://data.mendeley.com/datasets/2gsj2krvzb/1

Funding

This research was funded by a Knowledge Economy Skills Scholarship (KESS 2), which is part-funded by the Welsh Government's European Social Fund (ESF) convergence programme for West Wales and the Valleys, grant number AU30033. The KESS2 project sponsor was Pro-TEM Services Ltd. (UK), with contributions from Sona Nanotech (Canada).

Declaration of Competing Interest

The authors declare that they have no known competing financial interests or personal relationships that could have appeared to influence the work reported in this paper.

Acknowledgments

The authors gratefully acknowledge Helen Phillips for assisting with the FIE-HRMS analysis.

Appendix A. Supplementary data

Supplementary data to this article can be found online at https://doi.org/10.1016/j.rvsc.2022.09.001.

References

Ariel, O., Gendron, D., Dudemaine, P.L., Gevry, N., Ibeagha-Awemu, E.M., Bissonnette, N., 2020. Transcriptome profiling of bovine macrophages infected by Mycobacterium avium subspecies paratuberculosis depicts foam cell and innate immune tolerance phenotypes. Front. Immunol. https://doi.org/10.3389/fimmu.2019.02874.

Aschenbach, J.R., Kristensen, N.B., Donkin, S.S., Hammon, H.M., Penner, G.B., 2010. Gluconeogenesis in dairy cows: the secret of making sweet milk from sour dough. IUBMB Life. https://doi.org/10.1002/iub.400.

Barratt, A.S., Arnoult, M.H., Ahmadi, B.V., Rich, K.M., Gunn, G.J., Stott, A.W., 2018. A framework for estimating society's economic welfare following the introduction of an animal disease: the case of Johne's disease. PLoS One. https://doi.org/10.1371/journal.pone.0198436.

Beckmann, M., Parker, D., Enot, D.P., Duval, E., Draper, J., 2008. High-throughput, nontargeted metabolite fingerprinting using nominal mass flow injection electrospray mass spectrometry. Nat. Protoc. https://doi.org/10.1038/nprot.2007.500.

Bell, A.W., 1995. Regulation of organic nutrient metabolism during transition from late pregnancy to early lactation. J. Anim. Sci. https://doi.org/10.2527/1995.7392804x.

Benedictus, G., Verhoeff, J., Schukken, Y.H., Hesselink, J.W., 2000. Dutch paratuberculosis programme history, principles and development. Vet. Microbiol. https://doi.org/10.1016/S0378-1135(00)00325-4.

Biemans, F., Romdhane, R.B., Gontier, P., Fourichon, C., Ramsbottom, G., More, S.J., Ezanno, P., 2021. Modelling transmission and control of Mycobacterium avium subspecies paratuberculosis within Irish dairy herds with compact spring calving. Prev. Vet. Med. https://doi.org/10.1016/j.prevetmed.2020.105228.

Borst, P., 2020. The malate–aspartate shuttle (Borst cycle): how it started and developed into a major metabolic pathway. IUBMB Life. https://doi.org/10.1002/iub.2367.

Butot, S., Ricchi, M., Sevilla, I.A., Michot, L., Molina, E., Tello, M., Russo, S., Arrigonia, N., Garrido, J.M., Tomas, D., 2019. Estimation of performance characteristics of analytical methods for Mycobacterium avium subsp. paratuberculosis detection in dairy products. Front. Microbiol. https://doi.org/10.3389/fmicb.2019.00509.

Chong, J., Wishart, D., Xai, J., 2019. Using MetaboAnalyst 4.0 for comprehensive and integrative metabolomics data analysis. Curr. Prot. Bioinform. https://doi.org/10.1002/cpbi.86.

Costa, A., Lopez-Villalobos, N., Sneddon, N.W., Shalloo, L., Franzoi, M., De Marchi, M., Penasa, M., 2019. Invited review: Milk lactose - current status and future challenges in dairy cattle. J. Dairy Sci. https://doi.org/10.3168/jds.2018-15955.

De Buck, J., Shaykhutdinov, R., Barkema, H.W., Vogel, H.J., 2014. Metabolomic profiling in cattle experimentally infected with Mycobacterium avium subsp. paratuberculosis. PLoS ONE. https://doi.org/10.1371/journal.pone.0111872.

Donat, K., Soschinka, A., Erhardt, G., Brandt, H.R., 2014. Paratuberculosis: decrease in milk production of german holstein dairy cows shedding *Mycobacterium avium* Ssp. Paratuberculosis depends on within-herd prevalence. Anim. https://doi.org/10.1017/S1751731114000305.

Foroutan, A., Fitzsimmons, C., Mandal, R., Piri-Moghadam, H., Zheng, J., Guo, A.C., Li, C., Guan, L.L., Wishart, D.S., 2020. The bovine metabolome. Metabolites. https://doi.org/10.3390/metabo10060233.

Frey, P.A., 1996. The Leloir pathway: a mechanistic imperative for three enzymes to change the stereochemical configuration of a single carbon in galactose. FASEB J. https://doi.org/10.1096/fasebj.10.4.8647345.

Geraghty, T., Graham, D.A., Mullowney, P., More, S.J., 2014. A review of bovine Johne's disease control activities in 6 endemically infected countries. Prev. Vet. Med. https://doi.org/10.1016/j.prevetmed.2014.06.003.

Gerrard, Z.E., Swift, B.M.C., Botsaris, G., Davidson, R.S., Hutchings, M.R., Huxley, J.N., Rees, C.E.D, 2018. Survival of *Mycobacterium avium* subspecies *paratuberculosis* in retail pasteurised milk. Food Micro. https://doi.org/10.1016/j.fm.2018.03.004.

Hu, H., Fang, Z., Mu, T., Wang, Z., Ma, Y., Ma, Y., 2021. Applications of metabolomics in diagnosis of cow mastitis: A review. Front. Vet. Sci. https://doi.org/10.3389/fvets.2021.747519.

Hutjens, M.F., Sweeney, P.L.H., McNamara, J.P., 2016. Dry-lot dairy cow breeds. In: Encyclopedia of dairy sciences, (3rd ed.). Academic press, Cambridge, pp. 234–241.

Jurkovich, V., Bognár, B., Balogh, K., Kovács-Weber, M., Fornyos, K., Szabó, R.T., Kovács, P., Könyve, L., Mézes, M., 2016. Effects of subclinical Mycobacterium avium ssp. paratuberculosis infection on some physiological parameters, health status and production in dairy cows. Acta Vet. Hung. https://doi.org/10.1556/004.2016.029.

Luangwilai, M., Duangmal, K., Chantaprasarn, N., Settachaimongkon, S., 2021. Comparative metabolite profiling of raw milk from subclinical and clinical mastitis cows using 1H-NMR combined with chemometric analysis. Int. J. Food. Sci. Tech. https://doi.org/10.1111/ijfs.14665.

Martínez-Reyes, I., Chandel, N.S., 2020. Mitochondrial TCA cycle metabolites control physiology and disease. Nat. Comms. https://doi.org/10.1038/s41467-019-13668-3.

McNees, A.L., Markesich, D., Zayyani, N.R., Graham, D.Y., 2015. Mycobacterium paratuberculosis as a cause of Crohn's disease. Expert Rev Gastroenterol Hepatol. https://doi.org/10.1586/17474124.2015.1093931.

Micheluccia, A., Cordesa, T., Ghelfia, J., Pailota, A., Reilingb, N., Goldmannc, O., Binza, T., Wegnera, A., Tallama, A., Rausella, A., Buttinia, M., Linstera, C.L., Medinac, E., Ballinga, R., Hillera, K., 2013. Immune-responsive gene 1 protein links metabolism to immunity by catalyzing itaconic acid production. PNAS. https://doi.org/10.1073/pnas.1218599110.

Nielson, S.S., Toft, N., 2008. Ante mortem diagnosis of paratuberculosis: A review of accuracies of ELISA, interferon-γ assay and faecal culture techniques. Vet. Microbiol. https://doi.org/10.1016/j.vetmic.2007.12.011.

Nielson, S.S., Toft, N., 2012. Effect of days in milk and milk yield on testing positive in milk antibody ELISA to Mycobacterium avium subsp. paratuberculosis in dairy cattle. Veterinary Vet. Immunol. Immunopathol. https://doi.org/10.1016/j.vetimm.2012.05.013.

Safer, B., Smith, C.M., Williamson, J.R., 1970. Control of the transport of reducing equivalents across the mitochondrial membrane in perfused rat heart. J. Mol. Cell. Cardiol. https://doi.org/10.1016/0022-2828(71)90065-4.

Scano, P., Carta, P., Ibba, I., Manis, C., Caboni, P., 2020. An untargeted metabolomic comparison of milk composition from sheep kept under different grazing systems. Dairy. https://doi.org/10.3390/dairy1010004.

Stabel, J.R., Bradner, L., Robbe-Austerman, S., Beitz, D.C., 2014. Clinical disease and stage of lactation influence shedding of Mycobacterium avium subspecies paratuberculosis into milk and colostrum of naturally infected dairy cows. J. Dairy Sci. https://doi.org/10.3168/jds.2014-8204.

Sweeney, R.W., 1996. Transmission of paratuberculosis. Veterinary Clinics of North America. Food Anim. Pract. https://doi.org/10.1016/s0749-0720(15)30408-4.

Tata, A., Pallante, I., Massaro, A., Miano, B., Bottazzzari, M., Fiorini, P., Dal Pra, M., Paganini Stefani, A., De Buck, J., Piro, R., Pozzato, N., 2021. Serum metabolomic profiles of paratuberculosis infected and infectious dairy cattle by ambient mass spectrometry. Front. Vet. Sci. https://doi.org/10.3389/fvets.2020.625067.

Taylor, E.N., Beckmann, M., Villarreal-Ramos, B., Vordermeir, H.-M., Hewinson, G., Rooke, D., Mur, L.A.J., Koets, A.P., 2021. Metabolomic changes in naturally MAP-infected heifers indicate immunologically related biochemical reprogramming. Metabolites. https://doi.org/10.3390/metabo11110727.

Taylor, E.N., Beckmann, M., Markey, B.K., Gordon, S.V., Hewinson, G., Rooke, D., Mur, L.A.J., 2022. Metabolomic changes in Mycobacterium avium subsp. paratuberculosis (MAP) challenged Holstein–Friesian cattle highlight the role of serum amino acids as indicators of immune system activation. Metabolomics. https://doi.org/10.1007/s11306-022-01876-w.

Thirunavukkarasu, S., de Silva, K., Begg, D.J., Whittington, R.J., Plain, K.M., 2015. Macrophage polarization in cattle experimentally exposed to Mycobacterium avium subsp. paratuberculosis. Pathog. Dis. https://doi.org/10.1093/femspd/ftv085.

Tong, J., Zhang, H., Zhang, Y., Xiong, B., Jiang, L., 2019. Microbiome and metabolome analyses of milk from dairy cows with subclinical Streptococcus agalactiae mastitis – potential biomarkers. Front. Microbiol. https://doi.org/10.3389/fmicb.2019.02547.

Vrieling, F., Kostidis, S., Spanik, H.P., Haks, M.C., Mayboroda, O.A., Ottenhof, T.H.M., Joosten, S.A., 2020. Analyzing the impact of *Mycobacterium tuberculosis* infection on primary human macrophages by combined exploratory and targeted metabolomics. Sci. Rep. https://doi.org/10.1038/s41598-020-62911-1.

Whitlock, R.H., Buergelt, C., 1996. Preclinical and clinical manifestations of paratuberculosis (including pathology). Vet. Clin. North Am. Food Anim. https://doi.org/10.1016/s0749-0720(15)30410-2.

Whittington, R., Donat, K., Weber, M.F., Nielson, S.S., Eisenberg, S., Arrigoni, N., Juste, R., Sáez, J.L., Dhand, N., Santi, A., Michel, A., Barkema, H., Kralik, P., Kostoulas, P., Citer, L., Griffin, F., Barwell, R., Moreira, M.A.S., Slana, I., et al., 2019.

Control of paratuberculosis: Who, why and how. In: A Review of 48 Countries. Vet. Res, BMC. https://doi.org/10.1186/s12917-019-1943-4.
Windsor, P.A., Whittington, R.J., 2010. Evidence for age susceptibility of cattle to Johne's disease. Vet. J. https://doi.org/10.1016/j.tvjl.2009.01.007.
Xu, W., Vervoot, J., Saccenti, E., van Hoeij, R., Kemp, B., van Knegsel, A., 2018. Milk metabolomics data reveal the energy balance of individual dairy cows in early lactation. Sci. Rep. https://doi.org/10.1038/s41598-018-34190-4.
Xu, W., Vervoot, J., Saccenti, E., Kemp, B., van Hoeij, R.J., van Knegsel, A.T.M., 2020. Relationship between energy balance and metabolic profiles in plasma and milk of dairy cows in early lactation. J. Dairy Sci. https://doi.org/10.3168/jds.2019-17777.
Ying, W., 2006. NAD+ and NADH in cellular functions and cell death. Front. Biosci. https://doi.org/10.2741/2038.
Zhang, G., Zwierzchowski, G., Mandal, R., Wishart, D.S., Ametaj, B.N., 2020. Serum metabolomics identifes metabolite panels that differentiate lame dairy cows from healthy ones. Metabolomics. https://doi.org/10.1007/s11306-020-01693-z.